LAWRENCE
LIVERMORE
NATIONAL
LABORATORY

LLNL-TR-408750

Electrochemical NOx Sensor for Monitoring Diesel Emissions

L. Y. Woo, R. S. Glass

November 17, 2008

Disclaimer

This work performed under the auspices of the U.S. Department of Energy by Lawrence Livermore National Laboratory under Contract DE-AC52-07NA27344.

LLNL-TR-408750

Agreement 8697 - Electrochemical NO_x Sensor for Monitoring Diesel Emissions

Leta Y. Woo, and Robert S. Glass
Lawrence Livermore National Laboratory
P.O. Box 808, L-367
Livermore, CA 94551-9900
(925) 423-7140; fax: (925) (422-5844); e-mail: glass3@llnl.gov

DOE Technology Manager: Jerry L. Gibbs
(202) 586-1182; fax: (202) 586-1600; e-mail: jerry.gibbs@ee.doe.gov

Contractor: Lawrence Livermore National Laboratory, Livermore, California
Prime Contract No.: W-7405-Eng-48

Objectives

- Develop an inexpensive, rapid-response, high-sensitivity and selective electrochemical sensor for oxides of nitrogen for compression-ignition, direct-injection (CIDI) exhaust gas monitoring
- Explore and characterize novel, effective sensing methodologies based on impedance measurements
- Explore designs and manufacturing methods that could be compatible with mass fabrication
- Effectively collaborate with industry so that the technology can (ultimately) be transferred to a supplier and commercialized

Approach

- Use an ionic (O^{2-}) conducting ceramic as a solid electrolyte and metal or metal-oxide electrodes
- Correlate NO_x concentration with changes in impedance by measuring the cell response to an ac signal
- Evaluate sensing mechanisms using electrochemical techniques
- Characterize aging mechanisms and the effects on long-term performance of candidate sensor materials
- Understand and develop methodology to eliminate interferences
- Collaborate with the Ford Research Center to optimize sensor materials, operating parameters, and performance and perform dynamometer on-vehicle testing

Accomplishments

- Characterized sensing mechanisms responsible for impedancemetric NO_x sensing
- Improved sensor design by incorporating an alumina heated substrate which then allowed the development of an advanced prototype sensor that was packaged into a commercial oxygen sensor housing
- Successfully performed engine dynamometer testing on prototype sensors at Ford facilities demonstrating comparable performance with the only commercially-available NO_x sensor (but that does not meet cost, sensitivity, response time, and system architecture goals)
- Published two journal articles, presented a talk at the 32nd International Conference & Exposition on Advanced Ceramics and Composites, and gave an oral presentation to USCAR during their visit to LLNL in April

Future Direction

- Develop advanced prototypes using processes suitable for cost-effective, mass manufacturing
- Evaluate performance of prototypes, including long-term stability and cross-sensitivity, in laboratory, dynamometer, and on-vehicle tests
- Initiate the technology transfer process to a commercial entity

Introduction

Increasingly stringent emissions regulations will require the development of advanced gas sensors for a variety of applications. For example, compact, inexpensive sensors are needed for detection of regulated pollutants, including hydrocarbons (HCs), CO, and NO_x, in automotive exhaust. Of particular importance will be a sensor for NO_x to ensure the proper operation of the catalyst system in the next generation of diesel (CIDI) automobiles.

Because many emerging applications, particularly monitoring of automotive exhaust, involve operation in harsh, high-temperature environments, robust ceramic-oxide-based electrochemical sensors are a promising technology. Sensors using yttria-stabilized zirconia (YSZ) as an oxygen-ion-conducting electrolyte have been widely reported for both amperometric and potentiometric modes of operation.[1,2] These include the well-known exhaust gas oxygen (EGO) sensor.

More recently, ac impedance-based (i.e., impedancemetric) sensing techniques using YSZ have been reported for sensing water vapor, hydrocarbons, CO, and NO_x.[3-6] Typically small-amplitude alternating signal is applied, and the sensor response is measured at a specified frequency. Most impedancemetric techniques have used the modulus (or magnitude) at low frequencies (< 1 Hz) as the sensing signal and attribute the measured response to interfacial phenomena.[3-5] Work by our group has also investigated using phase angle as the sensing signal at somewhat higher frequencies (10 Hz).[6,7] The higher frequency measurements would potentially allow for reduced sampling times during sensor operation.

Another potential advantage of impedancemetric NO_x sensing is the similarity in response to NO and NO_2 (i.e., total-NO_x sensing).[3,4,6,7] Potentiometric NO_x sensors typically show higher sensitivity to NO_2 than NO, and responses that are opposite in sign. However, NO is more stable than NO_2 at temperatures > 600°C, and thermodynamic calculations predict ~90% NO, balance NO_2.[8] Since automotive exhaust sensors will probably be required to operate at temperatures > 600°C, NO is the dominant component in thermodynamic equilibrium and the target NO_x species. Also, the use of upstream catalysts could further promote the conversion of NO_x species to NO. Therefore, the focus of current work is to investigate the response to NO. Nevertheless, minimizing the sensitivity to a variety of competing species is important in order to obtain the accuracy necessary for achieving the emission limits.

Mitigating the effect of interfering gases (e.g., O_2, water vapor, HCs, etc.) is an area of current study. For impedancemetric NO_x sensors, our previous work has demonstrated that the cross-sensitivity to O_2 may be accounted for by comparing measurements at multiple frequencies.[6] Other strategies for compensation are also being explored, including calibration using data from existing sensors located nearby.

Our current work has made significant advances in terms of developing prototype sensors more suitable for commercialization. Also, dynamometer testing has provided real-world sensor performance data that will be useful in approaching potential suppliers to whom we can transfer the technology for commercialization. The advances are a direct result of understanding the sensing mechanisms responsible for impedance-based NO_x sensing and the effect of materials choice and sensor design/geometry.

Background

Previously, we reported the impedance response of a symmetric Au/YSZ/Au cell to O_2 and NO_x.[7] Both electrodes were exposed to the same gaseous environment (i.e., no reference gas) and constant spring-loaded pressure was used to maintain contact between cell components. For real-world sensor applications, spring-loaded devices are obviously not practical. Nevertheless, the early prototypes were used to initially explore the impedancemetric sensing mechanisms, which resulted in improvements to the sensor design and a platform that did not require spring-loaded pressure.

Impedance-based sensing requires that at least one of the two electrodes act as the "sensing" electrode and provides flexibility in sensor design, which can be either symmetric or asymmetric. Both the electrode composition and microstructure were shown to alter sensitivity, and general criteria for appropriate electrode materials were developed.[9]

Since sensitivity was found to rely on parallel contributions from the NO_x and O_2 reactions occurring at the electrode/electrolyte interface, the rate-determining step for the O_2 reaction needs to be controlled to yield the desired sensitivity to NO_x. In this regard, we have found that the parameters we have under our control are composition and microstructure .[9] NO_x sensitivity relies on electrodes with low

catalytic activity towards oxygen, which can be obtained by creating a dense microstructure and choosing compositions that have limited interaction with oxygen.

Figure 1 illustrates the impedancemetric NO_x sensing mechanisms using simplified steps for the electrochemical redox reactions. The actual redox reactions likely involve a much more complex series of steps (e.g., adsorption of gas species, transport along surfaces, electron transfer, diffusion of products away from reaction sites, etc.). Nevertheless, the illustration provides a summary of the important mechanisms involved.

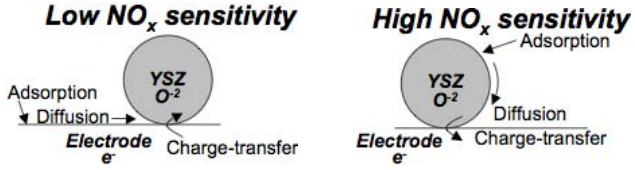

Figure 1. Illustration of simplified steps involved in impedancemetric NO_x sensing for (a) low NO_x sensitivity and (b) high NO_x sensitivity.

In the case of low NO_x sensitivity (Fig. 1a), processes proceed on electrodes with better oxygen catalytic activity so that the oxygen reaction rate dominates and controls the response; changes associated with variations in much lower concentration levels of NO_x are unable to be resolved. For high NO_x sensitivity (Fig. 1b), due to the poor oxygen catalytic activity of the electrode, processes can proceed on the electrolyte so that the NO_x reactions are able to compete with those of oxygen, and variation in ppm levels of NO_x can be resolved.

A number of materials potentially meet the sensing criteria, including gold and electronically conducting oxides. The current work builds on the previous findings by focusing on two different material systems and incorporating sensor designs more suitable for commercialization.

Experimental

Two different sensor prototypes were investigated. The first prototype was built on a dense alumina substrate (10 mm × 10 mm × 0.5 mm). Platinum paste was applied to the substrate and fired at 1200°C. Yttria-stabilized zirconia (YSZ) slurry was then applied on top of the fired Pt. Gold wire was tightly wrapped around the prototype and additional YSZ slurry was applied on top of the wires

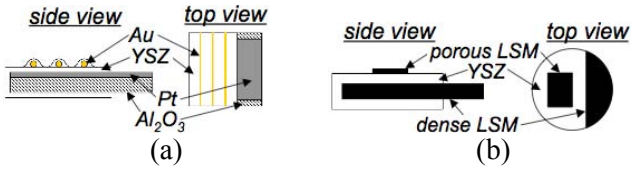

Figure 2. Schematic of NO_x prototype sensors based on (a) Pt/YSZ/Au cell and (b) LSM_{dense}/YSZ/LSM_{porous} cell.

and fired at 1000°C. Figure 2a shows a schematic of the Pt/YSZ/Au cell prototype.

The second prototype was built using a dense electronically conducting oxide substrate, strontium-doped lanthanum manganite (LSM). A dense pellet was prepared with commercial (Praxair) nominal $(La_{0.85}Sr_{0.15})_{0.98}Mn$ oxide powder by pressing in a uniaxial die and sintering at 1250°C. YSZ slurry was applied on top of the dense LSM, followed by LSM slurry, and fired at 1000°C. Fig. 2b shows a schematic of the LSM_{dense}/YSZ/LSM_{porous} cell prototype.

Gas sensing experiments were performed in a quartz tube placed inside a tube furnace with both electrodes exposed to the same environment. Gas composition was controlled in laboratory testing by mixing air, N_2, and a 1000 ppm NO/NO_2 feed using a standard gas handling system equipped with thermal mass flow controllers. Electrochemical measurements were performed using a Solartron 1260 Impedance Analyzer with a Solartron 1287 Electrochemical Interface.

Dynamometer testing of actual diesel exhaust was performed at Ford Research Center using an engine test cell fitted with a urea-based selective catalytic reduction (SCR) system for reducing NO_x emissions. Data were obtained using a constant engine speed, and the exhaust gas composition was altered using variations in the frequency of urea injection in the SCR system and the percent throttle. The exhaust gas composition, including CH_4, NO, NO_2, NH_3, CO, CO_2, and H_2O, was determined using Fourier Transform Infrared (FTIR) spectroscopy, and O_2 concentration was determined using a paramagnetic oxygen analyzer. The test setup also included a commercially available NO_x sensor located downstream of the prototype. Electrochemical measurements were performed using a stand-alone Solartron 1260 Impedance Analyzer.

Results and Discussion

Sensing Behavior of Prototypes

The Pt/YSZ/Au prototype is a significant improvement over previous sensor platforms by incor-

porating an alumina substrate. A commercializable sensor platform will need to include a heated substrate, which typically consists of an alumina substrate with Pt resistive heating elements. Figure 3 shows the impedancemetric sensing behavior for the Pt/YSZ/Au prototype at 650°C in laboratory testing. The sensing signal is the phase angle response of the cell to a 25 mV ac signal at 10 Hz.

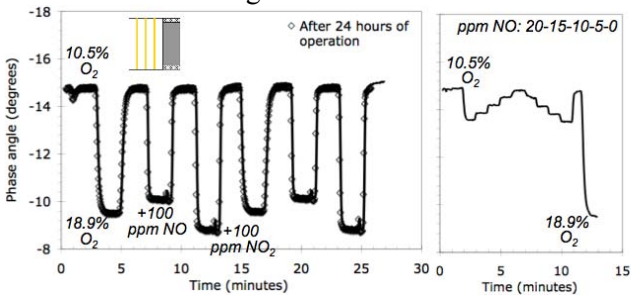

(a) (b)

Figure 3. Sensing behavior of Pt/YSZ/Au prototype at 650°C with changes in oxygen concentration and (a) 100 ppm additions of either NO or NO_2 or (b) response to step changes of 5 ppm NO up to 20 ppm. The sensing signal shown is the phase angle response of the cell to a 25 mV ac signal at 10 Hz.

In Fig. 3a, the background oxygen concentration was initially 10.5%, was then stepped to 18.9%, and the sensor response then recorded upon introduction of alternating concentrations of 100 ppm of NO and NO_2. For all changes in gas concentration, the sensor responds quickly and recovers quickly to the original baseline value (< 10 sec). Furthermore, introducing 100 ppm NO or NO_2 produces a similar type response to changing the oxygen concentration by 8.4%, which demonstrates that the sensor is much more sensitive to NO_x than oxygen. Also, in Fig. 3a the open data points represent data taken after 24 hours of operation, which agree well with the original data (shown as the solid line) and demonstrate sensor stability.

In impedancemetric sensing, NO and NO_2 have similar directional responses, which is an advantage over typical potentiometric sensors where NO and NO_2 have opposite signals that cancel. For the prototype shown in Fig. 3, the response to NO_2 is slightly larger than the response to NO, and will be discussed in further detail below. Also, in Fig. 3b, the Pt/YSZ/Au prototype response is shown for 5 ppm changes up to 20 ppm. The high-sensitivity prototype sensor clearly resolves 5 ppm changes in NO (that is, the sensitivity of the sensor is in the ppm range).

The $LSM_{dense}/YSZ/LSM_{porous}$ prototype is also an improvement over previous sensor designs because it demonstrated impedancemetric NO_x sensing using only high-temperature, potentially more stable materials. For a commercializable sensor platform, a single high-temperature co-firing process is desirable to minimize manufacturing costs. Furthermore, a platform that only utilizes high-temperature ceramics with similar thermal expansion coefficients should improve long-term thermal stability and resist degradation by thermal cycling.

Figure 4 shows the impedancemetric sensing behavior for the $LSM_{dense}/YSZ/LSM_{porous}$ prototype at 575°C in laboratory testing, using the same testing protocol shown in Fig. 3 and discussed above for the Pt/YSZ/Au prototype. The LSM prototype operated at 575°C has similar NO_x sensitivity to the Pt/YSZ/Au prototype operated at 650°C, as shown in Figs. 4a and 4b, and a lower sensitivity to oxygen.

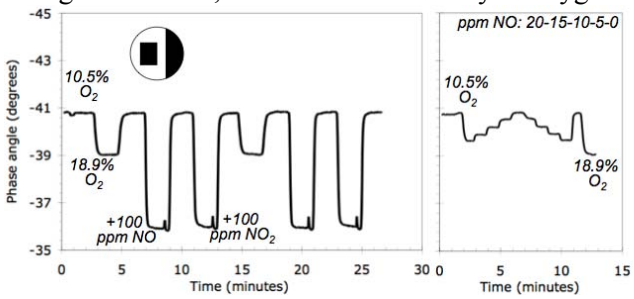

(a) (b)

Figure 4. Sensing behavior of $LSM_{dense}/YSZ/LSM_{porous}$ prototype at 650°C with changes in oxygen concentration and (a) 100 ppm additions of either NO or NO_2 or (b) response to step changes of 5 ppm NO up to 20 ppm.

The similarity in NO_x response for the two prototypes using different materials emphasizes that impedancemetric NO_x sensing is not restricted to a specific electrode material. Therefore, we can consider a variety of materials; however, microstructures, aging effects, sensor designs, and other considerations are still important.

Temperature-dependent NO_x sensitivity

Based on previous work investigating impedancemetric NO_x sensing mechanisms, the difference in operating temperatures to produce similar NO_x sensitivities for the two prototypes discussed above can be explained by the differing catalytic activities of the sensing electrode materials, Au vs. LSM.

For gas concentrations containing both O_2 and NO_x, the following redox reactions may occur at the electrode/electrolyte interface:

$$\frac{1}{2}O_2 + 2e^- \leftrightarrow O^{2-}$$
$$NO_2 + 2e^- \leftrightarrow NO + O^{2-} \quad (1)$$

For parallel contributions from the O_2 and NO_x reactions to the measured impedance, the relative rate constants for the two reactions would then determine the relative sensitivities to these gases. Sensing electrodes with low catalytic activity towards the oxygen reaction, and therefore higher rate constants for the NO_x reaction relative to the oxygen reaction, result in improved NO_x sensitivity.

In addition to an appropriate composition, previous work demonstrated that dense electrode microstructures were necessary to limit the oxygen reaction and obtain NO_x sensitivity.[9] For both of the asymmetric prototype sensors in our investigation, only one of the electrode/electrolyte interfaces dominates the measured sensitivity to NO_x. For the Pt/YSZ/Au prototype, the Au/YSZ interface provides the NO_x sensitivity, with Au serving as the sensing electrode; for the LSM prototype, only the dense LSM/YSZ interface influences NO_x sensing, with dense LSM serving as the sensing electrode.

At 650°C, the LSM prototype has very low NO_x sensitivity compared to the Pt/YSZ/Au prototype at the same temperature because LSM is more active towards oxygen catalysis than Au. However, reducing the operating temperature of the LSM prototype to 575°C lowers the catalytic activity and increases the NO_x sensitivity (relative reaction rate) of the dense LSM/YSZ interface.

NO vs. NO_2 Sensing Behavior

In addition to differences in operating temperature, the LSM prototype has identical responses to 100 ppm additions of either NO or NO_2. In comparison, the Pt/YSZ/Au prototype had a slightly larger response to NO_2. Gas phase equilibrium effects are proposed to explain the difference.

The following equation describes the relationship between oxygen, NO, and NO_2:

$$2NO_2(gas) \leftrightarrow 2NO(gas) + O_2(gas) \quad (2)$$

and can be used to calculate equilibrium values for NO and NO_2 using thermodynamic data for 10.5% O_2. At 575°C and 650°C, the equilibrium NO_x gas mixture has 87% and 93% NO, respectively.

For the LSM prototype, both NO and NO_2 have identical responses. The identical responses could indicate that the equilibrium NO_x concentration is presented to the sensing electrode. For the LSM prototype sensor design, the gas interacts with the porous LSM electrode before reaching the dense LSM/YSZ sensing interface. The porous LSM electrode likely provides enough catalytic activity for complete equilibrium of NO_x so that identical gas concentrations reach the sensing interface, regardless of whether the starting composition is NO or NO_2.

For the Pt/YSZ/Au prototype, NO_2 has a slightly larger response than NO indicating that the equilibrium NO_x concentration does not occur at the sensing electrode. For the Pt/YSZ/Au prototype sensor design, the gas only interacts with a thin layer of porous YSZ before reaching the Au/YSZ sensing interface. The porous YSZ does not provide the same catalysis as the porous LSM. Without a sufficient catalyst, additions of either NO or NO_2 will not result in identical equlibrium concentrations reaching the sensing interface.

Furthermore, in confirmation of this hypothesis, it was found that changing the thickness of the porous YSZ layer on the Pt/YSZ/Au sensor surface altered the response to either NO and NO_2. Figure 5a shows the impedance behavior for a Pt/YSZ/Au prototype with a single layer of porous YSZ on the sensor surface of approximately 50 to 100 μm thickness. The impedance behavior is shown on a Nyquist plot, which is a complex-plane plot with real impedance, Re(Z) plotted versus the negative imaginary impedance,-Im(Z).

In the Nyquist plot, each data point is taken at a different frequency, which increases from right to left; the darkened points and numbers correspond to log of frequency in Hertz. Features in the Nyquist plot, in particular the semicircular arcs, can be used to determine the contributions from interfacial and bulk phenomena to the overall impedance due to their appearance over a specific range of frequencies. The diameter of the individual arcs corresponds to real impedance (resistance) values.

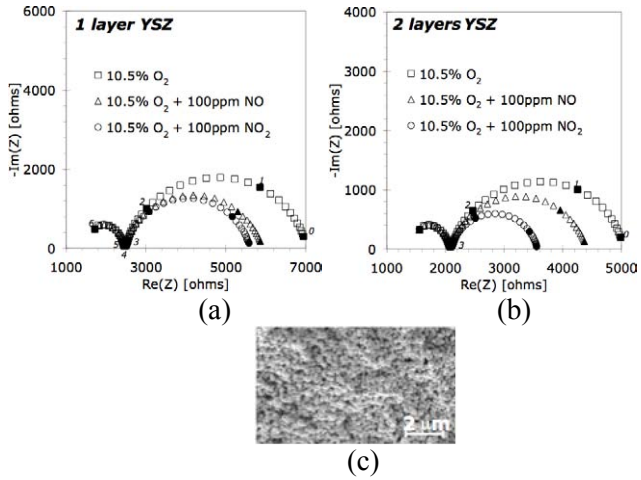

Figure 5. Nyquist plot of Pt/YSZ/Au prototype with (a) one layer and (b) two layers of YSZ slurry on the sensor surface at 650°C. (c) SEM picture of porous YSZ slurry.

In Fig. 5a, additions of either 100 ppm NO or NO_2 lead to similar changes in the impedance behavior. However, as the YSZ thickness is increased, as seen in Fig. 5b, additions of NO_2 cause a much larger decrease in impedance, as indicated by the larger decrease in the arc diameter, than additions of NO. Further increases in YSZ thickness with three and four layers (each layer was approximately 50 to 100 μm) did not cause any additional changes in the NO_2 vs. NO response; the overall electrode impedance continued to decrease.

The results from varying the thickness of the porous YSZ on the sensor surface indicate that the porous YSZ provides a more favorable pathway for NO_2, compared to NO, to the sensing interface. Figure 5c shows an SEM picture of the porous YSZ layer. For very thin layers of YSZ, there is limited interaction between the NO_x and the porous YSZ; all the gas introduced reaches the sensing interface without any changes in composition. Additions of NO and NO_2 respond similarly since for impedance-based sensing both the forward and reverse reactions are important.

As the porous YSZ thickness increases, the NO_x interacts with the porous YSZ surface before reaching the sensing interface. Our hypothesis is that the NO_2 has a faster diffusion pathway on the porous YSZ than in the gas phase; NO does not have a faster diffusion pathway on the porous YSZ. The effect of the faster surface diffusion for NO_2 only occurs within a limited distance from the sensing interface, and additional increases in thickness no longer produce additional increases in the NO_2 response relative to the NO response.

Previous results support our observation that NO_2 may have a faster diffusion path on the porous YSZ. For early prototypes using spring-loaded pressure, Au metal contacts were pressed against porous YSZ, a geometry that minimized interaction between NO_x and the porous YSZ. There would be minimal surface diffusion pathways on the YSZ available to NO_x before reaching the sensing interface, and a gas phase diffusion pathway would dominate. This early prototype, with minimal surface diffusion pathways on the YSZ, had almost identical responses to NO and NO_2.[7]

Additional investigation is necessary to fully understand the mechanisms responsible for the difference in behavior of NO and NO_2 in the Pt/YSZ/Au prototype. Nevertheless, we have demonstrated that controlling the thickness of the porous YSZ on the sensor surface can be used to create a total-NO_x sensor with similar responses to NO and NO_2.

Initial Long-term Stability Testing

Results from preliminary aging experiments indicate promising stability for meeting the accuracy and durability requirements, which are currently ±1 ppm and 10 yr/150k miles, respectively. The improved stability associated with impedance-based sensing compared with potentiometric or amperometric sensing could be due to the low-amplitude signals used, typically around 25 mV, which minimize any electrically driven changes. Furthermore, the use of alternating signals, as opposed to a constant dc signal, may prevent preferential aging effects at the interface associated with specific directional (i.e., cathodic or anodic) electrode reactions.

Figure 6a shows the sensing behavior for long-term aging of the Pt/YSZ/Au prototype at 650°C from 144 to 624 hours and indicates good reproducibility and minimal drift in the baseline and the response.

Figure 6b shows the sensing behavior for an LSM prototype similar to the one previously discussed, but the porous LSM electrode was replaced with Pt. However, the sensing interface (dense LSM/YSZ) is identical for both prototypes and should be suitable for comparison. The data shown in Fig. 6b were taken at 575°C with a background

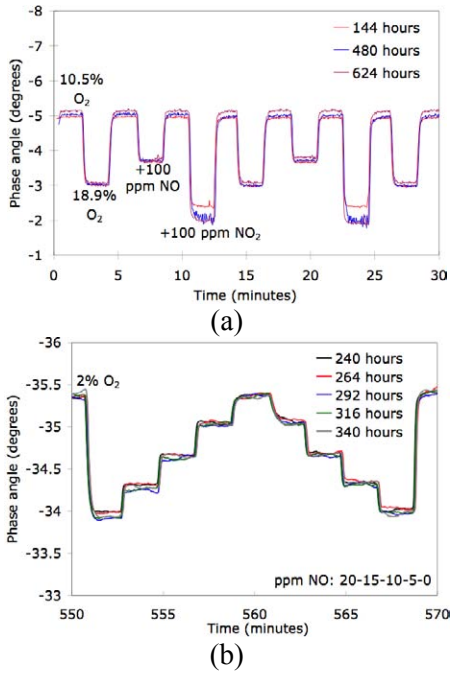

Figure 6. Sensing behavior of (a) Pt/YSZ/Au prototype at 650°C after long-term aging from 144 to 624 hours and (b) LSM_{dense}/YSZ/Pt prototype at 575°C after long-term aging from 240 to 340 hours.

oxygen concentration of 2% and step changes in the NO concentration up to 20 ppm total.

Initially, the LSM/YSZ/Pt prototype at 575°C showed a steady monotonic change in baseline signal before stabilizing after 240 hours of testing. The sensor signal remained stable for an additional 100 hours of testing, as shown in Fig. 6b, before again exhibiting monotonic changes in the baseline signal. The mechanism responsible for the baseline drift is likely microstructural changes in the Pt electrode, which has been shown previous work, and is currently being investigated.

Due to its excellent stability, the Pt/YSZ/Au prototype was selected for dynamometer testing in actual diesel exhaust at the Ford Research Center.

Dynamometer Testing

Engine dynamometer testing was performed on the Pt/YSZ/Au prototype using two different test sequences. The first sequence was designed to minimize changes in cross-interfering species, such as oxygen, while measuring the sensor response to changes in NO_x. Both the engine speed and throttle were held at constant values, 2750 rpm and 30%, respectively. Initially, excess urea was added to react with all the NO_x. The amount of urea was then reduced until all the urea reacted with the NO_x. Finally, the amount of urea was further reduced to produce varying levels of NO_x, as shown in Fig. 7.

In Fig. 7a, the raw sensor data from the prototype agrees reasonably well with data taken with the only currently available commercial NO_x sensor. (which, as previously noted does not fully meet automobile application requirements). The NO gas concentration measured by Fourier Transform Infrared (FTIR) spectroscopy is also shown for comparison in Fig. 7a.

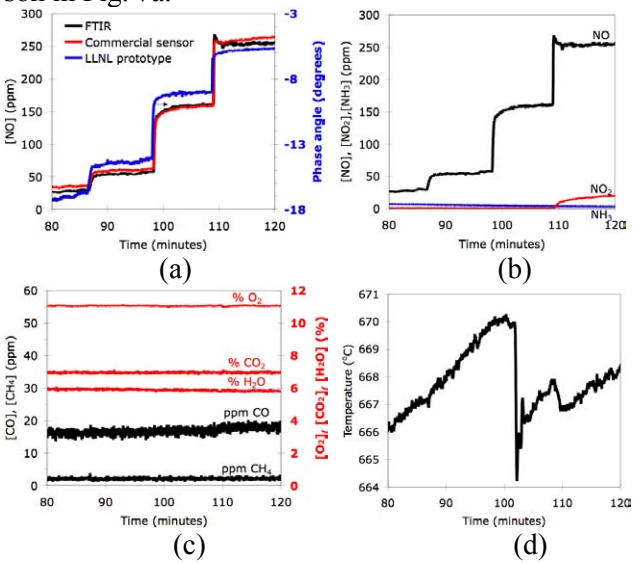

Figure 7. Dynamometer test results comparing (a) raw data from the Pt/YSZ/Au prototype with a commercial sensor and FTIR. (b) FTIR concentrations for NO, NO_2, and NH_3. (c) Constant values for CO, CH_4, CO_2, H_2O, and O_2. (d) Variations in temperature.

Additional data from FTIR and a paramagnetic oxygen analyzer, shown in Figs. 7b and 7c, demonstrate that NO is the primary species changing during the dynamometer test with low levels of NO_2, NH_3, CO, and CH_4. Also, O_2, CO_2, and H_2O remained constant during testing. Temperature measurements near the prototype, as shown in Fig. 7d, indicate fluctuations of around six degrees and do not correlate with trends seen in the prototype. Therefore, the measured changes in the prototype are a direct evaluation of its ability to detect changes in NO concentration in actual diesel exhaust.

The second test sequence was designed to investigate cross-interference from oxygen. The engine speed was held constant at 2750 rpm, with an initial throttle of 30%. Based on the first test sequence, enough urea was then introduced to minimize NO_x concentrations. Finally, the amount of throttle was

stepped to 40%, 35%, 32.5%, and 30% to vary gas concentrations, as shown in Fig. 8.

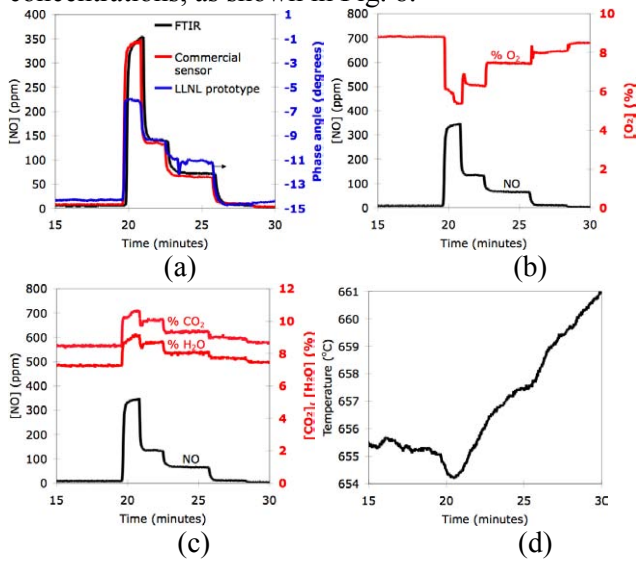

Figure 8. Dynamometer test results comparing (a) raw data from the Pt/YSZ/Au prototype with a commercial sensor and FTIR. Changes in (b) oxygen and (c) CO_2 and H_2O concentrations. (d) Variations in temperature.

In Fig. 8a, the general trend of the prototype agrees with the commercial sensor. However, the prototype no longer agrees in terms of relative response magnitudes, as measured in the first test sequence when interfering gases were minimized.

The second sequence also exhibited low levels of NO_2, NH_3, CO, and CH_4. However, O_2, CO_2, and H_2O no longer remained constant during testing when the percent throttle changed. Figure 8b shows a decrease in the oxygen concentration as throttle initially increased.

From laboratory testing, changes in oxygen concentration have a similar directional effect on the sensor signal as changes in NO_x concentration, although with much smaller sensitivities (see Fig. 3). Therefore, since the oxygen concentration is decreasing at the same time that the NO concentration is increasing, the combined effect is measured by the sensor. For the sensor signal, the decrease in oxygen concentration cancels out some of the signal associated with the increase in NO concentration.

The effect of oxygen interference is shown in Fig. 8a, where the prototype signal has a decreased response relative to the actual NO concentration increase (from 0 to 350 ppm) due to the simultaneous decrease in oxygen concentration from 9% to 6%. Changes in H_2O and CO_2 concentration are shown in Fig. 8c, and temperature fluctuations of around seven degrees are shown in Fig. 8d.

Previous work has demonstrated that the cross-sensitivity to oxygen may be accounted for by comparing measurements at multiple frequencies.[6] Other strategies for compensation are also being explored, including calibration using data from existing sensors located nearby. Cross-sensitivity studies are ongoing. The effectiveness of these strategies are currently being evaluated using the dynamometer results and will be published separately.

Commercializable Sensor Designs

The technology from the Pt/YSZ/Au prototype built on the alumina substrate was successfully transferred onto actual heated substrates provided by Ford. Initial sensing experiments for prototypes built on heated substrates agree reasonably well with data taken for the prototypes built on alumina substrates (without heating elements).

Additionally, the heated substrate prototypes were packaged into an oxygen sensor housing by a U.S. supplier, as shown in Fig. 9. Initial sensing experiments for the packaged Pt/YSZ/Au prototypes indicate reasonable sensitivity.

Figure 9. Photograph of Pt/YSZ/Au prototype built on a heated substrate and packaged into an oxygen sensor housing.

Both the incorporation of a heated substrate and an oxygen sensor housing indicates that the impedancemetric NO_x sensor technology can be adapted to a commercial sensor platform. In addition, utilizing these advanced sensor platforms removes the need for a furnace during testing. Additional laboratory and dynamometer testing are ongoing to evaluate the platforms.

Conclusions

Our work focused on two different impedancemetric NO_x sensor prototypes. Both demonstrate NO_x sensitivities to less than 5 ppm and response times of less than 10 seconds. Earlier prototypes have demonstrated response times of a few

second (< 5 sec.); however, the prototypes discussed here have not been optimized for response time. The advances in sensor development are a direct result of previous and current work characterizing impedancemetric NO_x sensing mechanisms based on YSZ-electrolyte cells.

The sensing mechanism depends on the porous YSZ/dense electrode interface, where only dense electrodes that are poor O_2 catalysts result in effective sensors. In impedancemetric sensing, either one or both electrodes can serve as the sensing electrode. The technology is not limited to a specific electrode material, and a number of materials potentially meet the sensing criteria, including gold and electronically conducting oxides, both of which were incorporated into prototypes in this study: Pt/YSZ/Au and LSM_{dense}/YSZ/LSM_{porous}.

Dynamometer engine testing in actual diesel exhaust was performed using appropriate test parameters in order to isolate the effect of NO_x. The sensing behavior of the prototype was compared alongside the only commercially-available NO_x sensor and a standard analytical FTIR instrument and demonstrated reasonable agreement.

Furthermore, advances toward a more commercializable sensor platform were achieved by incorporating a heated substrate. The heated substrate was also packaged into an oxygen sensor housing. Preliminary results show reasonable sensitivity from the advanced sensor platforms. Additional tests are ongoing.

References

1. F. Menil, V. Coillard, and C. Lucat, *Sensors and Actuators B* **67**, 1 (2000).
2. W. Göpel, G. Reinhardt and M. Rösch, *Solid State Ionics* **136–137**, 519 (2000).
3. N. Miura, M. Nakatou and S. Zhuiykov, *Ceram. Int.,* **30**, 1135 (2004).
4. N. Miura, M. Nakatou and S. Zhuiykov, *Sensors and Actuators B* **93**, 221 (2003).
5. N. Wu, Z. Chen, J. Xu, M. Chyu and S. X. Mao, *Sensors and Actuators B* **110**, 49 (2005).
6. L. P. Martin, L. Y. Woo, and R. S. Glass, *J. Electrochem. Soc.,* **154**, J97 (2007).
7. L. Y. Woo, L. P. Martin, R. S. Glass, and R. J. Gorte *J. Electrochem. Soc.,* **154**, J129 (2007).
8. J. Yoo, F. M. Van Assche, and E. D. Wachsman, *J. Electrochem. Soc.,* **153**, H115 (2006).
9. L. Y. Woo, L. P. Martin, R. S. Glass, W. Wang, S. Jung, R. J. Gorte, E. P. Murray, R. F. Novak, and J. H. Visser. *J. Electrochem. Soc.,* **155**, J32 (2008).

Publications/Presentations

"Investigating the stability and accuracy of the phase response for NO_x sensing 5% Mg-modified $LaCrO_3$ electrodes," *ECS Transactions*, **6**(20):43-62 (2007).

"Effect of electrode composition and microstructure on impedancemetric nitric oxide sensors based on YSZ electrolyte," *J. Electrochem. Soc.*, **155**(1):J32-J40 (2008).

Oral presentation made at the 32nd International Conference & Exposition on Advanced Ceramics and Composites, Jan. 27 – Feb. 1, 2008 in Daytona Beach, FL: "Sensing Mechanism of Impedancemetric NO_x Gas Sensors Based on Porous YSZ/Dense Electrode Interfaces."

Oral presentation entitled "NO_x Sensor Development for Monitoring Diesel Emissions" made during a visit by USCAR (United States Council for Automotive Research) to LLNL on April 23, 2008.